Journal of *Marine Science and Engineering*

MDPI

Article

Numerical Simulation of Vertical Cyclic Responses of a Bucket in Over-Consolidated Clay

Jun Jiang [1,2], Chengxi Luo [3] and Dong Wang [1,*]

[1] Shandong Engineering Research Center of Marine Exploration and Conservation, Ocean University of China, 238 Songling Road, Qingdao 266100, China; junjiang_hbcj@163.com
[2] School of Architectural Engineering, Hubei Urban Construction Vocational and Technological College, 28 Canglong Main Road, Wuhan 430205, China
[3] Power China Zhongnan Engineering Corporation Limited, Changsha 410014, China; luocx0150@126.com
* Correspondence: dongwang@ouc.edu.cn; Tel.: +86-13165325292

Abstract: Multi-bucket foundations have become an alternative for large offshore wind turbines, with the expansion of offshore wind energy into deeper waters. The vertical cyclic loading–displacement responses of the individual bucket of the tripod foundation are relevant to the deflection of multi-bucket foundations and crucial for serviceability design. Finite element analyses are used to investigate the responses of a bucket subjected to symmetric vertical cyclic loading in over-consolidated clay. The Undrained Cyclic Accumulation Model (UDCAM) is adopted to characterize the stress–strain properties of clay, the parameters of which are calibrated through monotonic and cyclic direct simple shear tests. The performance of the finite element (FE) model combined with UDCAM in simulating vertical displacement amplitudes is evaluated by comparison with existing centrifuge tests. Moreover, the impact of the bucket's aspect ratio on vertical displacement amplitude is investigated through a parametric study. A predictive equation is proposed to estimate the vertical displacement amplitudes of bucket foundations with various aspect ratios, based on the cyclic displacement amplitude of a bucket with an aspect ratio of unity.

Keywords: cyclic loading; bucket foundations; clay; offshore wind turbine; finite element method

Citation: Jiang, J.; Luo, C.; Wang, D. Numerical Simulation of Vertical Cyclic Responses of a Bucket in Over-Consolidated Clay. *J. Mar. Sci. Eng.* **2024**, *12*, 1319. https://doi.org/10.3390/jmse12081319

Academic Editor: José António Correia

Received: 3 July 2024
Revised: 27 July 2024
Accepted: 1 August 2024
Published: 4 August 2024

1. Introduction

Bucket foundations have been used in Europe and Asia to support offshore wind turbines [1]. Compared to the large-diameter monopile, the most popular foundation of a fixed wind turbine in shallow water, the bucket foundation can be used in deposits with shallow bedrocks and offers the advantage of easy installation [2,3]. Bucket foundations are classified into mono-bucket and multi-bucket types, with the latter typically consisting of three or four buckets [4]. Bucket foundations are designed to withstand large horizontal loads and overturning moments transmitted from the wind turbine and upper structures [5,6]. For multi-bucket foundations with bucket diameter of D, interactions between buckets are reasonably negligible, given that the spacing between them typically exceeds $3.5D$ in practice [7,8]. In this case, the moment transferred directly to the individual bucket is negligible in magnitude, and the displacement of the individual bucket is primarily caused by the cyclic tension–compression loading (Figure 1). Therefore, the serviceability of multi-bucket foundations is controlled by the cyclic vertical load–displacement responses of the individual buckets [9–11]. In addition to the movement of foundations under cyclic loading, the vibration of the tower under dynamical loading [12] and the structural stability under survival loads [13] are also essential for the design of offshore wind turbines, but are beyond the scope of this study.

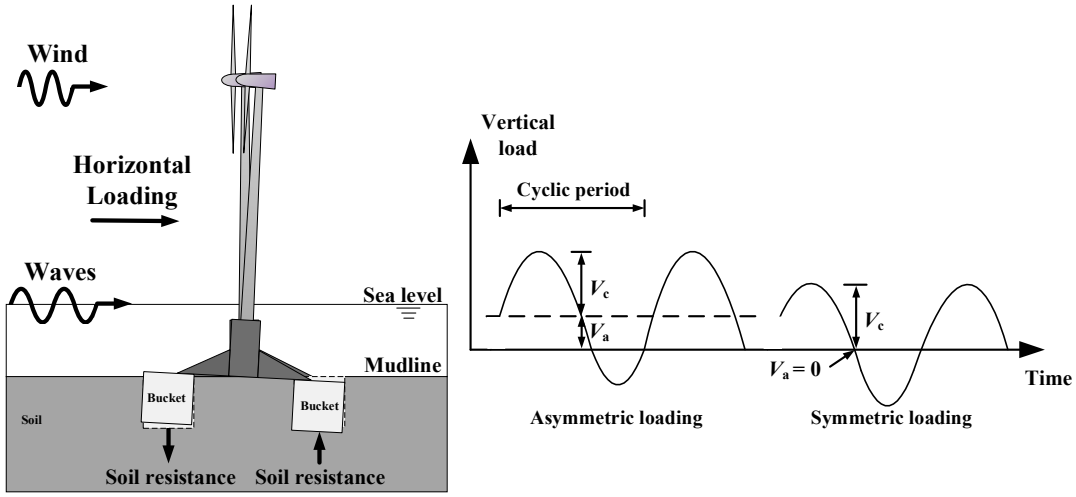

Figure 1. Response of multi-bucket foundation subjected to horizontal cyclic loading and definitions of vertical cyclic loading components.

To investigate the cyclic vertical displacements of a bucket in clay, conventional model tests [14,15] and model tests in centrifuge [16–18] have been conducted, where the bucket was usually displaced under nearly undrained conditions. Vertical cyclic loading was typically quantified through the vertical loading amplitude V_c and the average vertical loading V_a (Figure 1), causing the vertical displacement amplitude w_c and the average vertical displacement w_a. The accumulation of average vertical displacement and soil failure mechanisms depend on the direction of V_a; a zero or tensile V_a combined with arbitrary V_c value may lead to an upward w_a, which is more dangerous than the downward one [14,18,19]. Symmetric loading was the most dangerous condition since it would cause the most damaging strength loss [15,20]. Under symmetric loading with $V_a = 0$, the displacement amplitude w_c and average displacement w_a were both increased logarithmically with the number of cycles N, and the increases were more pronounced at higher V_c due to the more severe soil degradation [21]. However, a threshold of V_c may exist, below which the bucket is moved without significant accumulation of w_c and w_a after a large N [17,22].

Apart from the model tests, the cyclic responses of foundations in clay have been studied numerically [21,23]. The reliability of numerical results was dependent largely on whether the constitutive models could precisely describe the nonlinear response of soil under cyclic loading. Advanced constitutive models, such as the multi-surface model [23,24] and bounding surface model [18], have been developed to predict the displacements of foundations subjected to dozens of cycles [25]. However, the application of these models may be limited due to the large number of constitutive parameters and the potential computational errors accumulated during thousands of cycles [26]. An alternative option is the empirical approach simplifying the influence of a particular number of cycles through an equivalent static shear stress–strain relationship, e.g., the Undrained Cyclic Accumulation Model (UDCAM) that has been extensively used in practical applications over the last three decades [27–29]. In UDCAM, the cyclic shear strain contour diagrams are established via cyclic direct simple shear (DSS) tests or triaxial tests [30,31]. The program of UDCAM and the experimental database of a typical clay, Drammen clay [30], have been integrated into several commercial softwares, such as Bifurc [32] and Plaxis 3D Foundation Version 2.2 [33,34]. For other clays, the cyclic soil parameters can be determined from the existing database of Drammen clay [35]. The performance of UDCAM has been validated through comparisons with the model tests of gravity foundation [36,37] and then used to evaluate the undrained cyclic responses of monopiles [34]. Additionally, UDCAM was adopted in the design of monopiles in the Korean Western Sea, resulting in a more optimized solution than the conventional method recommended by the American Petroleum Institute [38,39].

However, it remains unclear whether UDCAM can be applied in the routine design of bucket foundations. As far as we know, the existing studies on the accumulation of vertical displacement amplitudes w_c of the bucket were mostly focused on a particular aspect ratio L/D (the ratio between skirt length L and diameter D of the bucket), for example, L/D of 0.5 in Zografou et al. [17] and 1 in Kou et al. [15]. The influence of L/D on w_c was quantified here.

In this paper, the responses of the individual bucket of the tripod foundation under symmetric cyclic vertical loading are investigated using finite element (FE) analyses. The cyclic properties of clay were represented by the UDCAM with shear strain contour diagrams. For verification of the numerical model, the simulated results of monotonic loading and cyclic loading tests for a bucket with aspect ratio L/D = 1 are compared with those obtained through centrifuge tests by Jiang et al. [18]. Subsequently, parameter analyses are conducted considering L/D ranging between 0.5 and 2, to investigate the effects of L/D on the simulated w_c. An equation is proposed to predict w_c for buckets with various L/D, based on the w_c of a bucket with L/D = 1. The validity of the proposed equation was further verified through additional cases featuring conditions beyond the scope of the parametric study. The process of the methodology is demonstrated in Figure 2.

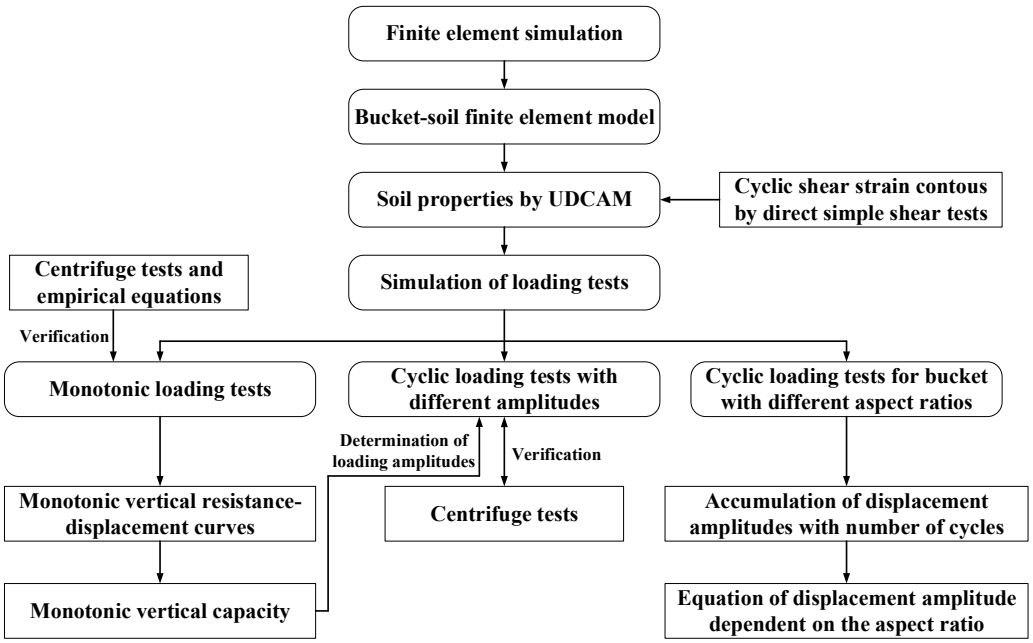

Figure 2. Process of the methodology.

2. Methodology

2.1. Finite Element Model

Commercial finite element package Plaxis 3D [33] was used to reproduce the interaction between the bucket and clay. The bucket was wished-in-place, whilst the installation effect was accounted for by reducing the shear stress along the skirt-soil interfaces with an adhesion factor [40,41]. The bucket diameter D was taken as 4 m (same as the bucket diameter in the prototype in Jiang et al. [18]), the skirt length L was 2, 4, 6, or 8 m, and skirt thickness was 0.1 m. The corresponding aspect ratios L/D were thus 0.5, 1, 1.5, and 2. Only half of the bucket and soil were modeled due to the symmetry of the foundation. The boundary conditions applied were as follows. Side surfaces of the soil were horizontally constrained and the soil base was fixed. The minimum and maximum aspect ratios selected, L/D = 0.5 and 2, were taken as examples and are shown in Figure 3. To avoid a boundary effect, the side edge of the soil was 3.4D away from the bucket skirt for all aspect ratios, while the soil bottom was 9L, 4L, 2.3L, and 1.5L away from the bucket tip at L/D = 0.5, 1, 1.5, and 2, respectively. Bucket and soil were discretized with ten-node tetrahedral

elements, with three degrees of freedom per node, referring to Banaszek et al. [42]. Four bucket–soil interfaces were set, including the ones outside and inside the bucket skirt and the ones below the cap and tip of the bucket. The interfaces were composed of twelve-node triangular interface elements formed by node pairs. One node of the pair belonged to the bucket and the other to soil. The shear stress of the interface was set as the undrained strength of the surrounding soil multiplied by an adhesion factor α. The value of α was calculated as $1/S_t$, where S_t denotes the soil sensitivity [10]. To meet the demands of convergence and accuracy, the coarseness factors of mesh were chosen as 0.1 for the bucket and soil inside the bucket, 0.3 for the soil near the bucket ($0.5D$ horizontally and at least $0.5L$ vertically away from the bucket, as the red doted lines shown in Figure 3), and 1 for the rest, as shown in Figure 3.

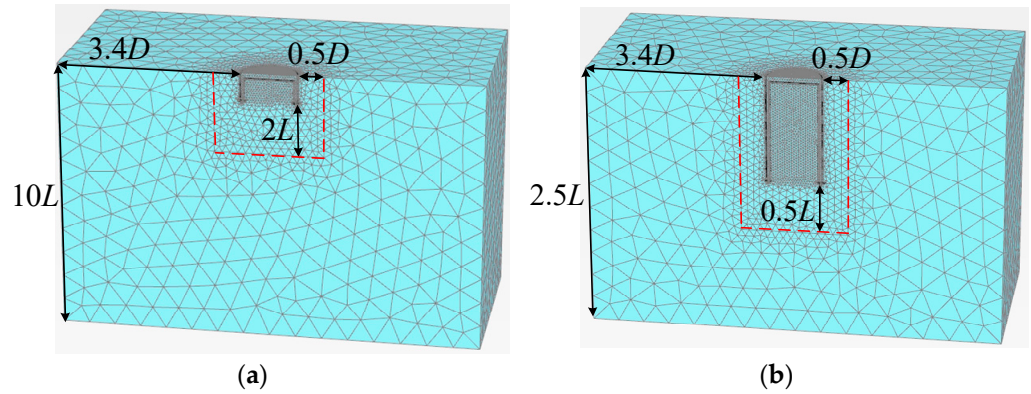

Figure 3. Mesh of the bucket and soil: (**a**) L/D = 0.5; (**b**) L/D = 2.

Total stress analyses were conducted, with clayey soil taken as undrained material. The bucket was simplified as a rigid body, with a reference point (RP) located at the center of the bucket cap. Consequently, the load–displacement responses of the bucket were characterized by the measurement at RP. Monotonic vertical loading tests were simulated using a displacement-controlled mode; vertical displacement w was applied at RP and the corresponding reaction force V was acquired. The vertical capacity of bucket V_0 was defined as the reaction force acquired when the vertical displacement reached quite a large value, for example, $0.25L$ adopted in Jiang et al. [18]. For cyclic vertical loading tests, a force-controlled mode was employed; the vertical loading amplitude V_c was applied at RP, leading to the corresponding displacement amplitude w_c. The specific values of V_c (expressed as the ratio between V_c and V_0) are shown in Table 1. At small w_c, the separation between bucket and soil interfaces was not allowed since suction was generated at the bucket base and the soil plug inside the bucket was moved along with it [18]. The simulations of large w_c, e.g., w_c between $0.1L$ and $0.25L$, were only considered in Section 3 for verification purposes, but not discussed in the parametric study due to the deflection limit of wind turbines in practice.

Table 1. Conditions of centrifuge tests by Jiang et al. [18].

Case	s_u (kPa)	V_c/V_0
1	6.5 + 0.55z	0.42
2	6.5 + 0.55z	0.53
3	11.6	0.58
4	9.0 + 0.4z	0.37
5	9.0 + 0.4z	0.51
6	6.0 + 0.18z	0.64

2.2. Soil Properties

The properties of clay used in centrifuge tests included the following: a specific gravity of 2.70, an effective unit weight of 6.97 kN/m^3, a liquid limit of 42.8, a plastic limit of 20.8, and a soil sensitivity, S_t, of 2.1. The UDCAM was used to characterize the cyclic shear stress–strain response of clay. For symmetric cyclic loading with $V_a = 0$, only symmetric DSS tests exhibiting an average shear stress $\tau_a = 0$ were required to form the cyclic strain contours, which describe the relationship between the cyclic stress τ_c, the cyclic strain γ_c, and the number of cycles N. The DSS tests were carried out following the standards ASTM D6528-17 [43]. With comprehensive details reported by Andersen [30], the procedure of implementing the UDCAM for the clay used in the centrifuge tests [18] is as follows:

(a) The slurry with water content twice the liquid limit was moved into a strongbox, and the soil sample was prepared under consolidation pressure of 60 or 90 kPa. The overburden pressure at the skirt tip level in centrifuge tests was around 30 kPa, corresponding to an over-consolidation ratio (OCR) of 2 or 3. Therefore, the specimen for DSS test was consolidated at vertical stress of 60 or 90 kPa. Then, the specimen was unloaded to 30 kPa prior to the following shearing.

(b) The prepared specimens underwent shearing at a displacement rate of 0.015 mm/min to obtain the monotonic shear stress–strain responses (τ-γ responses), as shown in Figure 4. As a result, the static undrained shear strength s_u was defined as the shear stress at γ = 15% [44]. Then, s_u = 18.3 kPa for OCR = 2 and s_u = 22.9 kPa for OCR = 3.

(c) In symmetric cyclic shearing tests, various stress ratio amplitudes τ_c/s_u ranging from 0.2 to 0.7 were adopted, and the frequency was chosen as 0.1 Hz to match the typical wave frequency. Contour diagrams that describe the τ_c/s_u-N response are derived by connecting the data points from test results at the same γ_c values, e.g., γ_c = 0.08%, 0.14%, 0.5%, 1%, 1.5%, 3%, and 15%, as illustrated in Figure 5a,b.

(d) For a symmetric cyclic loading scenario with a uniform loading amplitude, the equivalent number of cycles was equal to the current number of cycles N. The typical γ_c values varying with τ_c/s_u can be obtained by linking the intersection points of lines at N = 1, 10, 100, and 1000 with the contours in Figure 5. As a result, the τ_c/s_u-γ_c curves for OCR = 3 are shown in Figure 6 as an example. The response of τ_c/s_u-γ_c at another relevant N can be interpolated automatically in Plaxis.

(e) To derive the dimensional τ_c-γ_c response, the static undrained shear strength s_u was required. The strength profiles of clay samples were inferred from cone penetration tests, with the cone factor taken as 15 [18]. As shown in Table 1, the undrained strength of clay, s_u, was increased with the soil depth z for most soil types, while a uniform clay sample had a constant s_u. The soil depth z and s_u are in units of m and kPa, respectively.

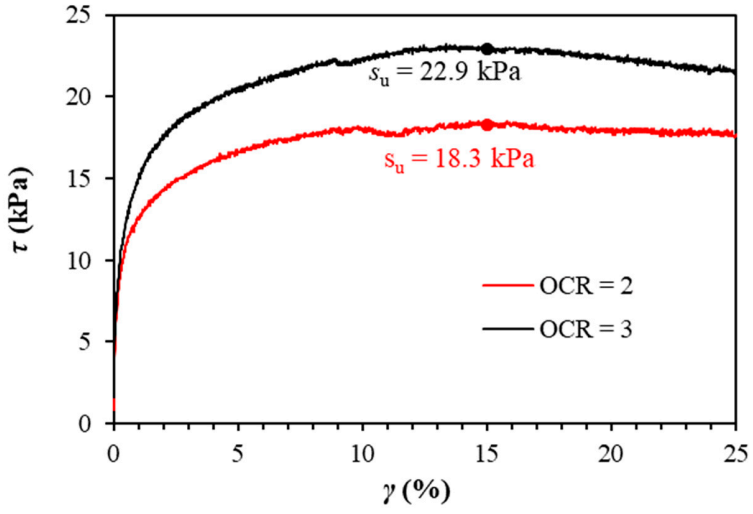

Figure 4. Static shear strength from monotonic DSS tests.

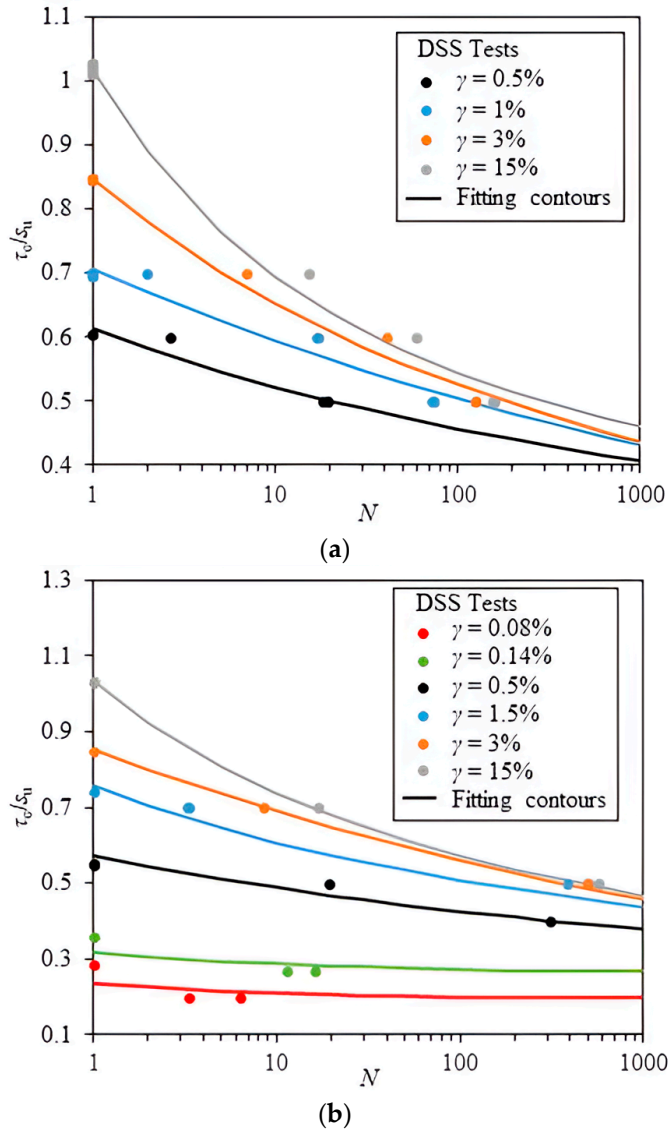

Figure 5. Contour diagrams at $\tau_a = 0$ deduced from cyclic DSS tests: (**a**) OCR = 2; (**b**) OCR = 3.

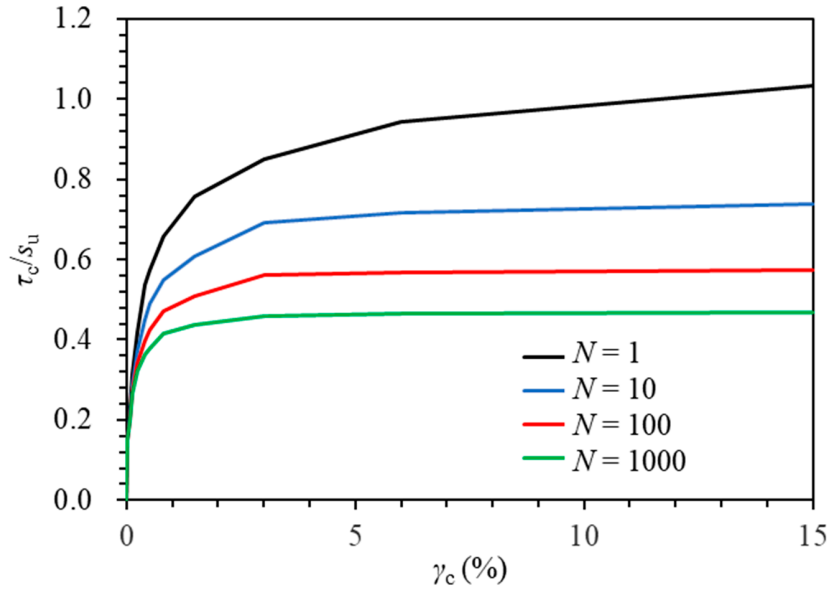

Figure 6. Typical γ_c values varying with τ_c/s_u at N = 1, 10, 100, and 1000 (OCR = 3).

3. Verification

3.1. Monotonic Loading Tests

To verify the reliability of the finite element model, monotonic vertical loading tests by Jiang et al. [18], named Tests 1-1, 2-1, 3-1, and 4-1 and carried out in four separate strongboxes, were simulated. Clay was regarded as a Tresca material under undrained conditions. The undrained shear strengths of clay samples were deduced from cone penetration tests. Specifically, $s_u = 6.5 + 0.55z$, 11.6, $9.0 + 0.4z$, and $6.0 + 0.18z$ for Samples 1–4, where soil depth z and s_u are in units of m and kPa, respectively. The adhesion factor α was set as $1/S_t = 0.5$, as the values of S_t in each strongbox are averaged as 2.1. A typical value of Young's modulus, $400s_u$, was adopted. The effective unit weight of clay γ_c' was 6.97 kN/m^3 and Poisson's ratio was taken as 0.495 to approximate constant volume under undrained conditions. The vertical force–displacement curves (V-w curves) of four tests by FE are shown in Figure 7. Similar to the centrifuge test results, the vertical force by FE increased rapidly with displacement at first, and then the increase trend became gentle. The vertical capacity V_0 of the bucket by FE was defined as the vertical reaction force V at vertical displacement $w = 0.25L$. V_0 by FE was very close to that by centrifuge tests. A simple equation was recommended in guidelines DNV RP E303 [45] to estimate the vertical force V:

$$V = z\alpha s_{ua}\pi D + (\gamma_c' z + s_{utip}N_c)A, \quad (1)$$

where A is the cross-section area of the bucket; s_{ua} is the average undrained shear strength along the bucket skirt; s_{utip} is the undrained shear strength at the bucket tip; N_c is the bearing capacity factor under plan strain conditions, usually taken as 7.5 [46]. The V_0 values in Equation (1) are presented as markers in Figure 7 for comparison purposes. The errors of V_0 values between FE and Equation (1) were less than 17%; it was reasonable for the reliability of the FE model [47], since the empirical equations were based on several simplifications.

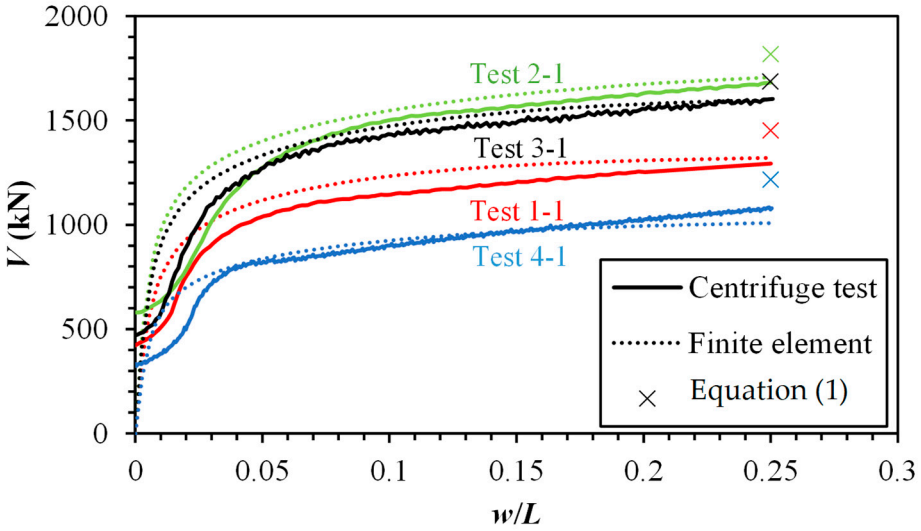

Figure 7. Monotonic vertical force–displacement curves from FE analyses and tests.

3.2. Cyclic Loading Tests

To further validate the FE model combined with UDCAM, six cyclic vertical loading tests with negligible V_a, named Tests 1-2, 1-3, 2-2, 3-2, 3-3, and 4-2 in Jiang et al. [18], were mimicked. Loading amplitudes for the six tests varied between $0.37V_0$ and $0.64V_0$, whereas the average loading values caused by the controlling error ranged from $0.01V_0$ to $0.05V_0$.

The cyclic vertical displacement amplitudes of the bucket w_c from centrifuge tests were normalized to the length of the bucket skirt L, represented by solid markers in Figure 8. Typical data points were used to illustrate the progression of w_c/L in relation to the number of cycles N throughout the tests, and the values of w_c/L exceeding $0.25L$ are not shown.

Observations indicated that w_c/L from centrifuge tests increased logarithmically with N. This phenomenon is attributed to the higher accumulation of pore pressure in centrifuge tests under larger N, consistent with the shear stress–strain curve at N = 1000, lower than that at N = 1, according to the DSS tests in Figure 6. The FE results of w_c/L are depicted as hollow markers in Figure 8. The predicted w_c/L exhibited a tendency similar to those observed in the centrifuge tests, highlighting the robustness of the UDCAM. For a low loading amplitude with V_c/V_0 = 0.37 or 0.42, the w_c/L values increased gently with the number of cycles in both centrifuge tests and FE simulations, and the bucket was actually under a stable state without significant accumulation of vertical displacement. As a comparison, a rapid failure of the bucket foundation was observed under a higher loading amplitude. For example, the failure occurred after 20 cycles with V_c/V_0 = 0.64 in the centrifuge, as demonstrated in Figure 8b, while the failure took place after 5 to 10 cycles in FE simulations. It was recognized that there existed divergences between the numerical and experimental data:

(a) At the early stage of loading, for example, N = 2, w_c/L predicted by the FE was lower than the measured value, and the divergence decreased with an increase in V_c/V_0. This phenomenon can be explained by the smaller cyclic shear strain at a lower cyclic shear stress given a certain number of cycles, as shown in Figure 6. As a result, w_c/L by centrifuge tests was larger at higher V_c/V_0 and more closely aligned with the simulations.

(b) Although the experimental w_c/L was higher than the value predicted by FE, the divergence became smaller with increasing cycles (e.g., V_c/V_0 = 0.37 and 0.51). In particular scenarios, V_c/V_0 = 0.42 at N > 650 and V_c/V_0 = 0.58 at N > 20, w_c/L measured in the tests appeared lower than the FE results. This phenomenon may be attributed to the potential consolidation effect which is caused by partial dissipation of pore pressures around the bucket during the long-term loading in centrifuge tests. For example, the loading duration amounted to 137 d in the prototype after 996 cycles with V_c/V_0 = 0.37, thereby allowing partially drained conditions in clay, which caused an increase in undrained shear strength and reduction in w_c/L. Conversely, the degradation of undrained strength induced by cyclic loading was accounted for in the UDCAM strategy, while the potential enhancement of undrained strength due to partial drainage within the long-term loading stage was ignored.

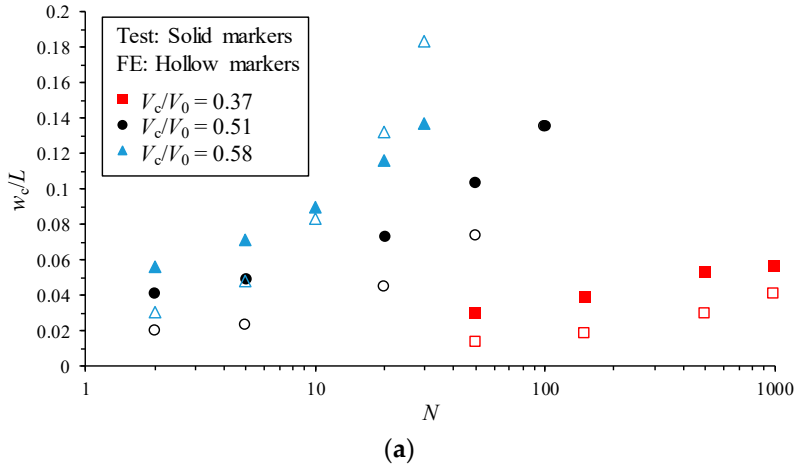

(**a**)

Figure 8. *Cont.*

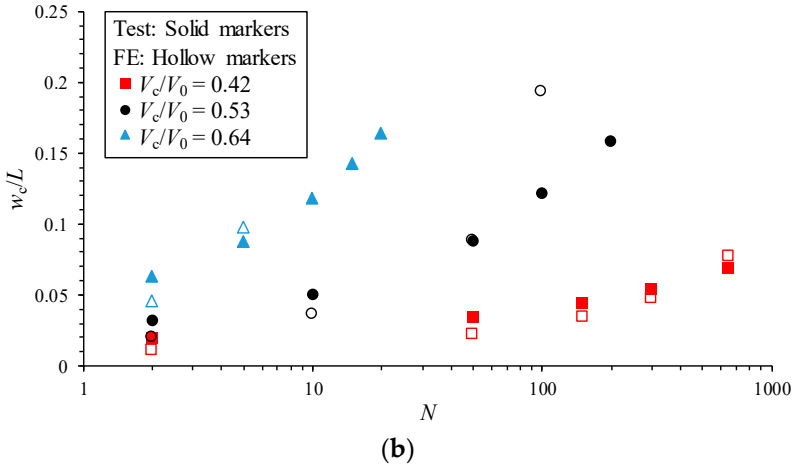

Figure 8. Comparison of cyclic displacement amplitudes by centrifuge test and FE: (**a**) V_c/V_0 = 0.37, 0.51, and 0.58; (**b**) V_c/V_0 = 0.42, 0.53, and 0.64.

4. Parametric Study

Various aspect ratios of the buckets with a diameter D of 4 m were employed in FE analyses to investigate the influence of the aspect ratio on w_c. The aspect ratio was 1 in the centrifuge tests by Jiang et al. [18], and here, it is changed to 0.5, 1.5, and 2, respectively. The FE results of two typical cases, Cases 1 and 3, are chosen to detail the findings. The combinations of clay properties and loading conditions of the two cases are listed in Table 1.

The vertical capacities V_0 against various aspect ratios need to be determined prior to simulating the vertical displacement amplitude w_c, by following the procedure addressed in Section 3.1. The V_0 values for Case 1 are 970.7, 1321.2, 1606.0, and 1897.3 kN against the aspect ratio of 0.5, 1, 1.5, and 2. For Case 3, V_0 values are identified as 1422.8, 1707.1, 1860.2, and 2024.3 kN for four aspect ratios, respectively.

According to the FE simulations combined with the UDCAM, w_c values under various numbers of cycles are predicted. As illustrated in Figure 9, w_c/L increases logarithmically with increasing N, but w_c/L is higher at lower L/D. The failure mechanisms of soil at various L/D values under cyclic loading, for instance, N = 300 for Case 1, are demonstrated in Figure 10. It is evident that the soil contained within the bucket moved along with the bucket, resulting in a reversed end bearing mechanism. The displacement of the mobilized soil in Figure 10 is larger with increasing L/D, resulting in an increased w_c of the bucket with increasing L/D. This trend is opposite to the decreased w_c/L with increasing L/D in Figure 9.

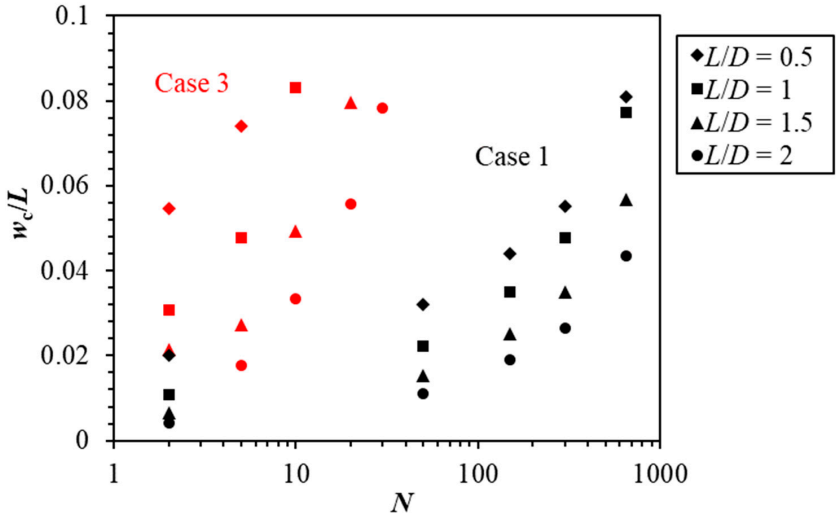

Figure 9. Comparison of cyclic loading amplitudes with N at different L/D values.

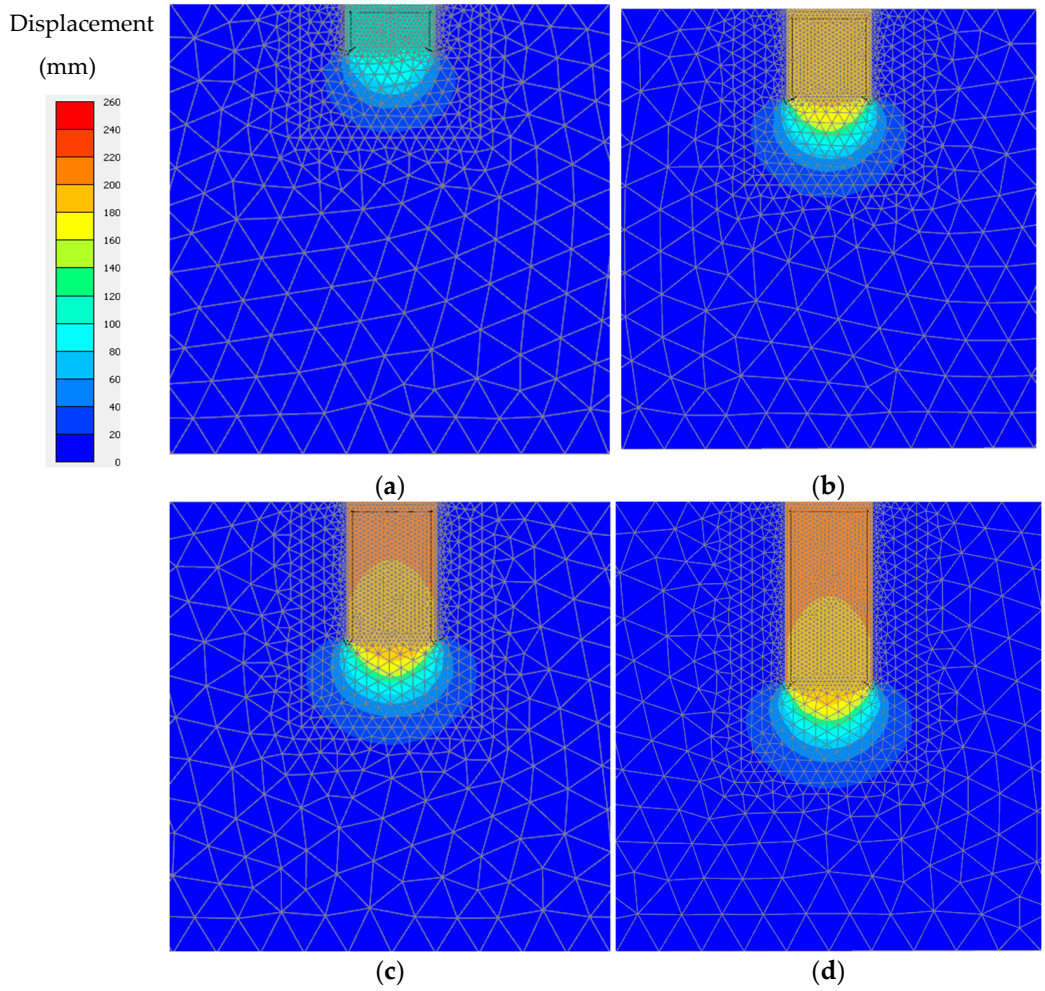

Figure 10. Displacement contours at N = 300 for Case 1: (**a**) L/D = 0.5; (**b**) L/D = 1; (**c**) L/D = 1.5; (**d**) L/D = 2.

By considering w_c/L at L/D = 1 as the reference displacement $(w_c/L)_{ref}$, w_c/L for varying L/D can be predicted using a fitting equation, as shown in Equation (2):

$$\frac{w_c/L}{(w_c/L)_{ref}} = 1 + 0.2\left(\frac{L}{D}\right)^2 \tanh\left[16.5\left(\frac{L}{D} - 1\right)\right] \quad (2)$$

The w_c/L values estimated by Equation (2) of the two cases are demonstrated in Figure 11. A reasonable agreement on w_c/L is achieved between the predictions of Equation (2) and FE results. The divergences for all cases are predominantly within the range of ±25%.

Despite reasonable agreement highlighted in Figure 11, it is not clear if Equation (2) is applicable for predicting w_c/L under the conditions beyond the scope of the above parametric study. The fatal factors include bucket sizes, undrained shear strengths and degradation behaviors of soil, the adhesion factors, and the amplitude of cyclic loading. Therefore, the reliability of Equation (2) is verified further through six additional cases listed in Table 2. In these six cases, the bucket diameter is selected deliberately as 2, 4, or 8 m to cover the practical applications. The aspect ratio of the bucket is extended to 3, as the aspect ratios of 0.5–2 are investigated already to deduce Equation (2). Two strength profiles representing undrained shear strength under over-consolidated and normally consolidated conditions are employed in Table 2. By following the recommendation of guidelines DNV-RP-E303 [45] and research by Shen et al. [41], the adhesion factor α is taken as 0.3 or 0.65, corresponding to the operation phases of immediately after the installation of the bucket and months or years after the installation of the bucket, respectively. The V_c/V_0

values are in the range of 0.3–0.58, to avoid the potential shakedown of the bucket under V_c/V_0 less than 0.3 or rapid failure of the bucket under V_c/V_0 larger than 0.58. It should be noted that V_0 values for the additional cases are determined using the same procedure addressed in Section 3.1. As a result, V_0 values are shown in the last column in Table 2.

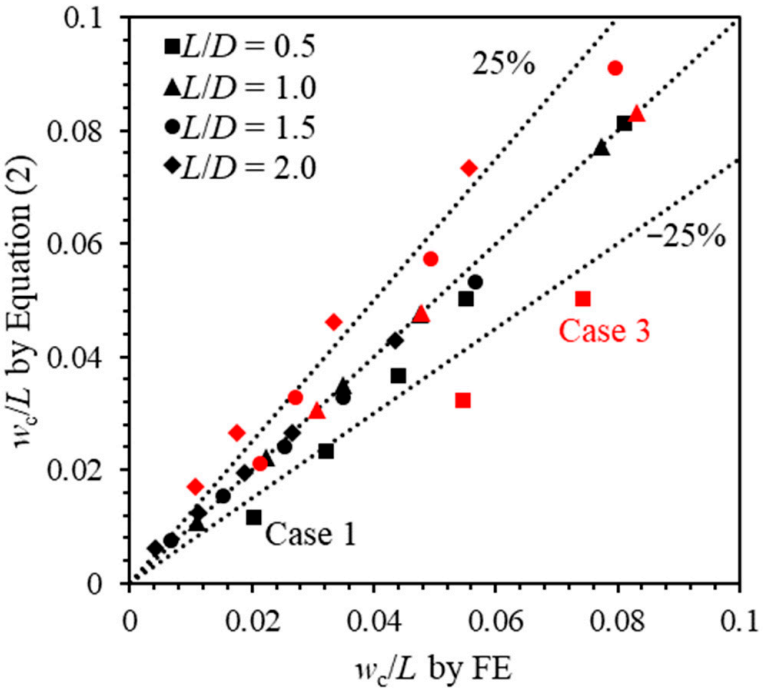

Figure 11. Comparison of w_c/L by FE and Equation (2) at D = 4 m and various L/D values.

Table 2. Additional cases for the reliability of Equation (2).

Case	D (m)	L/D	s_u (kPa)	α	V_c/V_0
A	8	0.5	6.5 + 0.55z	0.5	0.42
B	8	0.5	11.6	0.5	0.58
C	2	3	6.5 + 0.55z	0.5	0.42
D	2	3	11.6	0.5	0.58
E	4	1.5	30	0.65	0.30
F	4	1.5	10 + z	0.3	0.50

The w_c/L values by FE and Equation (2) are compared in Figure 12. It is evident in Figure 12a,b that Equation (2) is applicable for buckets with an aspect ratio ranging from 0.5 to 3 under the loading amplitudes considered, irrespective of the bucket diameter values. The w_c/L values predicted by Equation (2) are satisfactory in most cases, except for Case F in Figure 12c. A possible reason is that the clay in Case F is normally consolidated and the undrained shear strength increases more significantly with depth than that in other cases, whereas Equation (2) is more suitable for heavily over-consolidated soils with nearly uniform shear strength (s_u = 11.6 or 30 kPa) and slightly over-consolidated soils. Additionally, Equation (2) is valid for an adhesion factor ranging between 0.3 and 0.65, covering the typical operation phases of the bucket from the installation to a moderately long operational duration after the installation.

For practical application involving the predictions of w_c for buckets under symmetric vertical loading in clay using UDCAM, the following steps are suggested. (a) Establish the DSS cyclic strain contour diagrams through monotonic and cyclic DSS tests, to derive the normalized cyclic shear stress–strain relationship τ_c/s_u-γ_c. (b) Determine the static shear strength s_u through cone penetration tests. (c) Simulate w_c for a bucket with L/D = 1, utilizing the cyclic soil properties identified in Steps (a) to (c). (d) Calculate w_c for buckets

with relevant D and L/D using Equation (2). By employing the aforementioned steps, only a limited number of DSS tests, cone penetration tests, and numerical simulations are required to predict w_c for bucket foundations across various aspect ratios. This procedure is applicable for soils with different shear strengths and adhesion factors, and loading amplitudes V_c/V_0 in the range of 0.3–0.58.

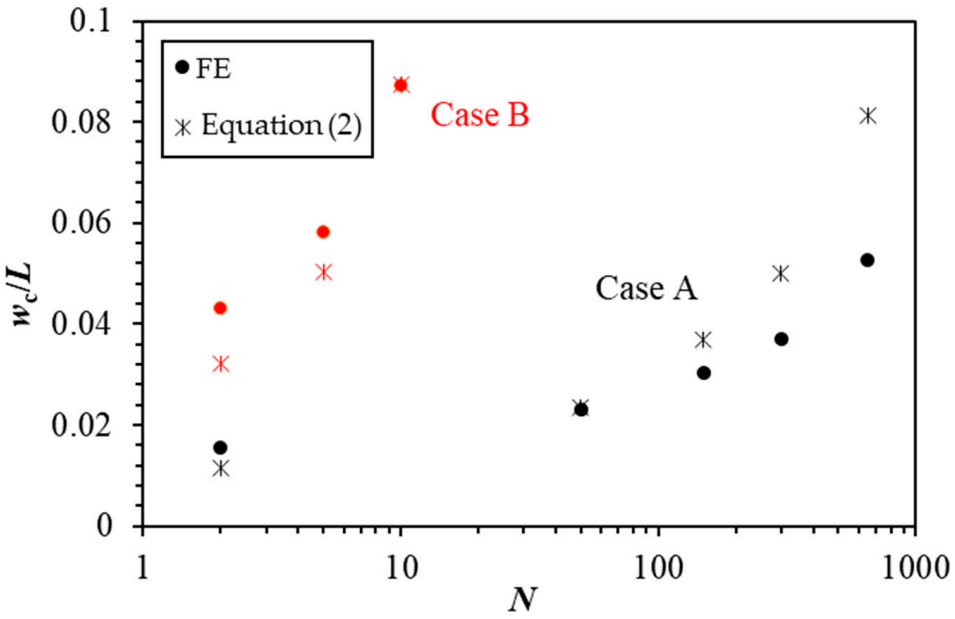

(**a**)

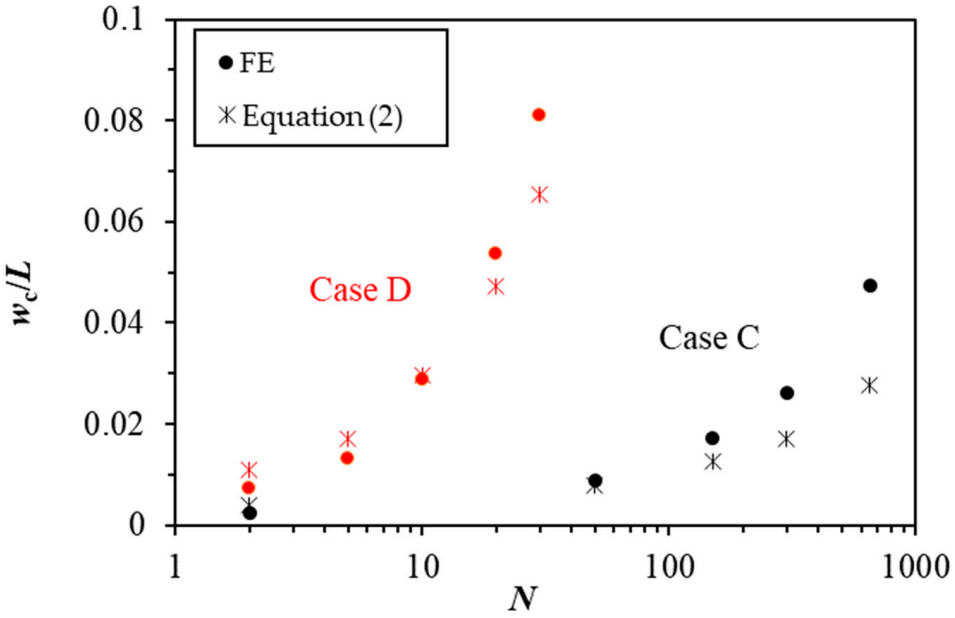

(**b**)

Figure 12. *Cont.*

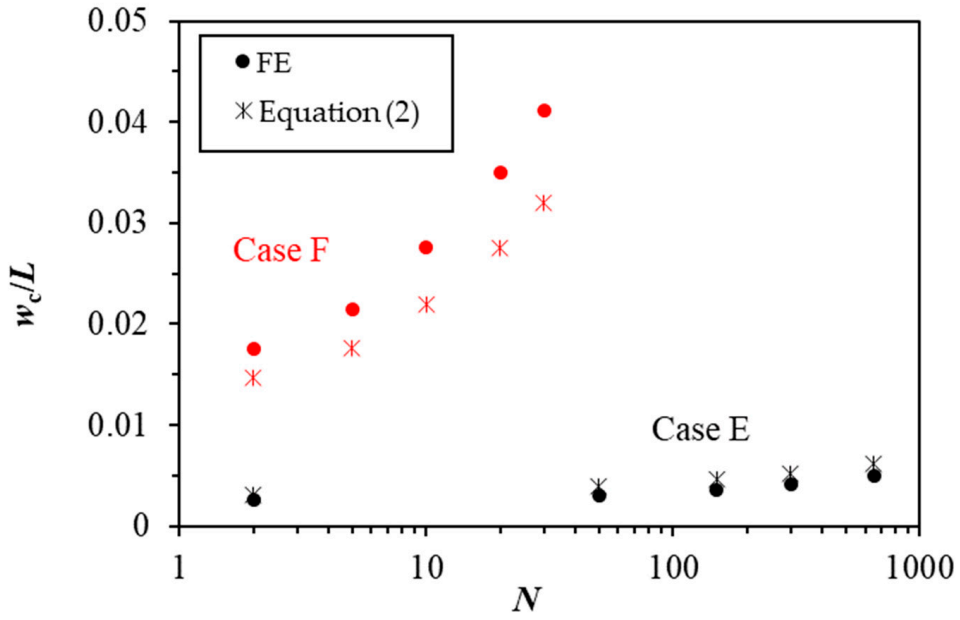

(**c**)

Figure 12. Performance of Equation (2) for cases in Table 2: (**a**) Cases A and B; (**b**) Cases C and D; (**c**) Cases E and F.

5. Conclusions

The accumulation of normalized vertical displacement amplitude w_c/L for buckets under symmetric vertical cyclic loading has been investigated through finite element (FE) analyses. Cyclic shear stress–strain relationships in clay are characterized using cyclic shear strain contour diagrams in a direct simple shear state. The results of w_c/L by FE are compared with those by centrifuge tests. In the parametric study, the aspect ratio L/D of the bucket is varied between 0.5 and 2 to investigate the effect of L/D on the prediction of w_c/L. The main conclusions are as follows:

(1) The w_c/L predicted by the FE model combined with UDCAM in this study exhibits reasonable agreement with the w_c/L obtained from existing centrifuge tests. The UDCAM is applicable for characterizing the cyclic shear stress–strain response of clay at a relevant number of cycles.

(2) The w_c/L in the parametric study decreases with increasing L/D. Taking w_c/L at L/D = 1 as a reference displacement, a predictive equation, Equation (2), for w_c/L at various L/D values has been proposed. It is proved that Equation (2) is applicable for buckets with L/D ranging between 0.5 and 3 and diameter D ranging between 2 and 8 m, normalized vertical loading amplitudes V_c/V_0 in the range of 0.3–0.58, and soil adhesion factors between 0.3 and 0.65. Equation (2) demonstrates better performance in soils with uniform or slightly increased undrained shear strength with depth than in soils with undrained shear strength increasing significantly with depth. In practical applications, a four-step procedure is suggested to predict w_c/L for bucket foundations across various aspect ratios, based on limited laboratory tests and FE simulations. The buckets with aspect ratios ranging between 0.5 and 3 are explored here, and the expansion of Equation (2) to larger aspect ratios needs to be testified in future. As for buckets under asymmetric vertical cyclic loading, the accumulation of w_c/L can be investigated through centrifuge tests at first and then compared with the predicted results by the proposed four-step procedure.

Author Contributions: Conceptualization, D.W., J.J. and C.L.; methodology, J.J.; software, D.W. and J.J.; validation, D.W. and J.J.; formal analysis, J.J.; investigation, J.J., D.W. and C.L.; data curation, J.J.; writing—original draft preparation, J.J.; writing—review and editing, D.W., C.L. and J.J.; funding acquisition, D.W. All authors have read and agreed to the published version of the manuscript.

Funding: This research was funded by the National Natural Science Foundation of China (grant Nos. 42025702 and 52394251).

Institutional Review Board Statement: Not applicable.

Informed Consent Statement: Not applicable.

Data Availability Statement: Data is contained within the article or supplementary material.

Conflicts of Interest: Author Chengxi Luo was employed by the company Power China Zhongnan Engineering Corporation Limited. The remaining authors declare that the research was conducted in the absence of any commercial or financial relationships that could be construed as a potential conflict of interest.

References

1. Bae, K.T.; Choo, Y.W.; Youn, H.; Kim, J.Y.; Choi, C.; Kwon, O. Geotechnical Perspective on Offshore Wind Plan, Strategy, Projects and Research in Korea. In Proceedings of the 19th International Conference on Soil Mechanics and Geotechnical Engineering: Technical Committee 209 Workshop, Seoul, Republic of Korea, 20 September 2017.
2. Houlsby, G.T.; Byrne, B.W. Suction Caisson Foundations for Offshore Wind Turbines and Anemometer Masts. *Wind Eng.* **2000**, *24*, 249–255. [CrossRef]
3. Zhu, F.Y.; O'Loughlin, C.D.; Bienen, B.; Cassidy, M.J.; Morgan, N. The Response of Suction Caissons to Long-Term Lateral Cyclic Loading in Single-Layer and Layered Seabeds. *Géotechnique* **2018**, *68*, 729–741. [CrossRef]
4. Faizi, K.; Faramarzi, A.; Dirar, S.; Chapman, D. Investigating the Monotonic Behaviour of Hybrid Tripod Suction Bucket Foundations for Offshore Wind Towers in Sand. *Appl. Ocean Res.* **2019**, *89*, 176–187. [CrossRef]
5. Achmus, M.; Kuo, Y.S.; Abdel-Rahman, K. Behavior of Monopile Foundations under Cyclic Lateral Load. *Comput. Geotech.* **2009**, *36*, 725–735. [CrossRef]
6. Petas, V.; Kolotsios, G.; Georgiadis, K.; Loukogeorgaki, E. Effect of Horizontal Loading on the Bearing Capacity of Tripod Skirted Foundations on Clay. In Proceedings of the 26th International Ocean and Polar Engineering Conference, Rhodes, Greece, 26 June 2016.
7. Zhao, Z.; Kouretzis, G.; Sloan, S.; Gao, Y. Ultimate Lateral Resistance of Tripod Pile Foundation in Clay. *Comput. Geotech.* **2017**, *92*, 220–228. [CrossRef]
8. Jeong, Y.H.; Kim, J.H.; Park, H.J.; Kim, D.S. Cyclic Behavior of Unit Bucket for Tripod Foundation System Supporting Offshore Wind Turbine via Model Tests. *Wind Energy* **2019**, *22*, 257–268. [CrossRef]
9. Kim, D.J.; Choo, Y.W.; Kim, J.H.; Kim, S.; Kim, D.S. Investigation of Monotonic and Cyclic Behavior of Tripod Suction Bucket Foundations for Offshore Wind Towers Using Centrifuge Modeling. *J. Geotech. Geoenviron. Eng.* **2014**, *140*, 04014008. [CrossRef]
10. He, B.; Jiang, J.; Cheng, J.; Zheng, J.; Wang, D. The Capacities of Tripod Bucket Foundation under Uniaxial and Combined Loading. *Ocean Eng.* **2021**, *220*, 108400. [CrossRef]
11. Carbon Trust. *Suction Installed Caisson Foundations for Offshore Wind: Design Guidelines*, 1st ed.; Carbon Trust: London, UK, 2019; pp. 1–92.
12. Elias, S.; Beer, M. Vibration Control and Energy Harvesting of Offshore Wind Turbines Installed with TMDI under Dynamical Loading. *Eng. Struct.* **2024**, *315*, 118459. [CrossRef]
13. Zakir, M.N.; Abasin, A.R.; Irshad, A.S.; Elias, S.; Yona, A.; Senjyu, T. Practical Wind Turbine Selection: A Multicriterion Decision Analysis for Sustainable Energy Infrastructure. *Pract. Period. Struct. Des. Constr.* **2024**, *29*, 04024028. [CrossRef]
14. Villalobos, F.A.; Byrne, B.W.; Houlsby, G.T. Model Testing of Suction Caissons in Clay Subjected to Vertical Loading. *Appl. Ocean Res.* **2010**, *32*, 414–424. [CrossRef]
15. Kou, H.; Fang, W.; Zhou, N.; Huang, J.; Zhang, X. Dynamic Response of Single-Bucket Foundation in Clay under Vertical Variable Amplitude Cyclic Loadings. *Ocean Eng.* **2023**, *273*, 113973. [CrossRef]
16. Chen, W.; Randolph, M.F. Uplift Capacity of Suction Caissons under Sustained and Cyclic Loading in Soft Clay. *J. Geotech. Geoenviron. Eng.* **2007**, *133*, 1352–1363. [CrossRef]
17. Zografou, D.; Gourvenec, S.; O'Loughlin, C. Vertical Cyclic Loading Response of Shallow Skirted Foundation in Soft Normally Consolidated Clay. *Can. Geotech. J.* **2019**, *56*, 473–483. [CrossRef]
18. Jiang, J.; Wang, D.; Fu, D. Vertical Monotonic and Cyclic Responses of a Bucket in Over-Consolidated Clay. *J. Mar. Sci. Eng.* **2023**, *11*, 2044. [CrossRef]

19. Randolph, M.F. Offshore Design Approaches and Model Tests for Sub-Failure Cyclic Loading of Foundations. In *Mechanical Behaviour of Soils under Environmentally Induced Cyclic Loads*; Di Prisco, C., Wood, D.M., Eds.; CISM Courses and Lectures; Springer: Vienna, Austria, 2012; pp. 441–480, ISBN 978-3-7091-1068-3.
20. Randolph, M.; Gourvenec, S. *Offshore Geotechnical Engineering*; CRC Press: London, UK, 2017; ISBN 978-1-315-27247-4.
21. Cheng, X.; Yang, A.; Li, G. Model Tests and Finite Element Analysis for the Cyclic Deformation Process of Suction Anchors in Soft Clays. *Ocean Eng.* **2018**, *151*, 329–341. [CrossRef]
22. Iskander, M.; El-Gharbawy, S.; Olson, R. Performance of Suction Caissons in Sand and Clay. *Can. Geotech. J.* **2002**, *39*, 576–584. [CrossRef]
23. Houlsby, G.T.; Abadie, C.N.; Beuckelaers, W.J.A.P.; Byrne, B.W. A Model for Nonlinear Hysteretic and Ratcheting Behaviour. *Int. J. Solids Struct.* **2017**, *120*, 67–80. [CrossRef]
24. Abadie, C. Cyclic Lateral Loading of Monopile Foundations in Cohesionless Soils. Ph.D. Thesis, University of Oxford, Oxford, UK, 2015.
25. Liu, H.; Pisanò, F.; Jostad, H.P.; Sivasithamparam, N. Impact of Cyclic Strain Accumulation on the Tilting Behaviour of Monopiles in Sand: An Assessment of the Miner's Rule Based on SANISAND-MS 3D FE Modelling. *Ocean Eng.* **2022**, *250*, 110579. [CrossRef]
26. Houlsby, G.T.; Kelly, R.B.; Huxtable, J.; Byrne, B.W. Field Trials of Suction Caissons in Clay for Offshore Wind Turbine Foundations. *Géotechnique* **2005**, *55*, 287–296. [CrossRef]
27. Andersen, K.H. Bearing Capacity under Cyclic Loading—Offshore, along the Coast, and on Land. *Can. Geotech. J.* **2009**, *46*, 513–535. [CrossRef]
28. Jostad, H.; Grimstad, G.; Andersen, K.; Saue, M.; Shin, Y.; You, D. A FE Procedure for Foundation Design of Offshore Structures—Applied to Study a Potential OWT Monopile Foundation in the Korean Western Sea. *Geotech. Eng.* **2014**, *45*, 63–72.
29. Zhang, C.; Wang, D.; Zheng, J. A Cyclic-Softening Macro Element Model for Mono-Bucket Foundations Supporting Offshore Wind Turbines in Clay. *Comput. Geotech.* **2023**, *161*, 105603. [CrossRef]
30. Andersen, A. Cyclic Soil Parameters for Offshore Foundation Design. In Proceedings of the 3rd International Symposium on Frontiers in Offshore Geotechnics, Oslo, Norway, 10 June 2015.
31. Skau, K.S.; Chen, Y.; Jostad, H.P. A Numerical Study of Capacity and Stiffness of Circular Skirted Foundations in Clay Subjected to Combined Static and Cyclic General Loading. *Géotechnique* **2018**, *68*, 205–220. [CrossRef]
32. Jostad, H.; Andresen, L. A FE Procedure for Calculation of Displacement and Capacity of Foundations Subject to Cyclic Loading. In Proceedings of the 1st International Symposium on Computational Geomechanics, Juan les Pins, France, 29 April 2009.
33. Manuals-PLAXIS-GeoStudio | PLAXIS Wiki-GeoStudio | PLAXIS-Bentley Communities. Available online: https://communities.bentley.com/products/geotech-analysis/w/wiki/46137/manuals---plaxis (accessed on 23 April 2024).
34. Khoa, H.D.V.; Jostad, H.P. Application of a Cyclic Accumulation Model UDCAM to FE Analyses of Offshore Foundations. In Proceedings of the 4th Congrès International de Géotechnique—Ouvrages-Structures, Ho Chi Minh City, Vietnam, 26 October 2017.
35. Andersen, K.H.; Engin, H.K.; D'Ignazio, M.; Yang, S. Determination of Cyclic Soil Parameters for Offshore Foundation Design from an Existing Data Base. *Ocean Eng.* **2023**, *267*, 113180. [CrossRef]
36. Skau, K.S.; Jostad, H.P. Application of the NGI-Procedure for Design of Bucket Foundations for Offshore Wind Turbines. In Proceeding of the 24th International Ocean and Polar Engineering Conference, Busan, Republic of Korea, 15 June 2014.
37. Rasch, C. Modelling of Cyclic Soil Degradation: Development of a Cyclic Accumulation Model and the Application to a Gravity Based Foundation. Master's Thesis, Delft University of Technology, Delft, The Netherlands, 2016.
38. API RP 2GEO Geotechnical and Foundtaion Design Considerations. Available online: https://www.intertekinform.com/en-au/standards/api-rp-2geo-2011-add-1-2014-97863_saig_api_api_206786/ (accessed on 3 July 2024).
39. Jostad, H.; Grimstad, G.; Andersen, K.; Sivasithamparam, N. A FE procedure for calculation of cyclic behaviour of offshore foundations under partly drained conditions. In Proceedings of the 3rd International Symposium on Frontiers in Offshore Geotechnics, Oslo, Norway, 10 June 2015.
40. Supachawarote, C. Inclined Load Capacity of Suction Caisson in Clay. Ph.D. Thesis, The University of Western Australia, Perth, Australia, 2006.
41. Shen, K.; Jiang, J.; Wang, D.; Zheng, J. Capacities of Tripod Bucket Foundation under Uniaxial and Combined Loading Considering Adhesion Factor. *Mar. Georesour. Geotechnol.* **2022**, *40*, 1520–1528. [CrossRef]
42. Banaszek, A.; Petrovic, R.; Zylinski, B. Finite Element Method Analysis of Pipe Material Temperature Changes Influence on Line Expansion Loops in Hydraulic Installations on Modern Tankers. *Therm. Sci.* **2011**, *15*, 81–90. [CrossRef]
43. *ASTM D6528-17*; Standard Test Method for Consolidated Undrained Direct Simple Shear Testing of Cohesive Soils. ASTM International: West Conshohocken, PA, USA, 2017.
44. Lunne, T.; Andersen, K.H. Soft clay shear strength parameters for deepwater geotechnical design. In Proceedings of the 6th International Offshore Site Investigation and Geotechnics Conference, London, UK, 11 September 2007.
45. DNV-RP-E303 Geotechnical Design and Installation of Suction Anchors in Clay. Available online: https://www.dnv.com/oilgas/download/dnv-rp-e303-geotechnical-design-and-installation-of-suction-anchors-in-clay/ (accessed on 3 July 2024).

46. Andersen, K.H.; Jostad, H.P. Foundation Design of Skirted Foundations and Anchors in Clay. In Proceedings of the 31st Offshore Technology Conference, Houston, TX, USA, 3 May 1999.
47. Wang, J.; Yang, H. Model Tests and Numerical Simulation on Bearing Capacity of Bucket Foundations in Soft Clay Under Vertical Static and Cyclic Loads. In Proceedings of the Seventeenth International Offshore and Polar Engineering Conference, Lisbon, Portugal, 1–6 July 2007; p. ISOPE-I-07-346.